EurJOC
European Journal of Organic Chemistry

Chemistry Europe
European Chemical Societies Publishing

Accepted Article

Title: Origins of the Reactivity in 1,3-Dipolar Cycloadditions of Acyl-isocyanide Ylides

Authors: Javier E. Alfonso-Ramos, Ruben Van Lommel, David Hernández-Castillo, Frank De Proft, Roy González-Alemán, Erik V. Van der Eycken, and Gerardo Manuel Ojeda Carralero

To be cited as: *Eur. J. Org. Chem.* **2022**, e202201028

Link to VoR: https://doi.org/10.1002/ejoc.202201028

WILEY-VCH

10.1002/ejoc.202201028

WILEY-VCH

RESEARCH ARTICLE

Origins of the Reactivity in 1,3-Dipolar Cycloadditions of Acyl-isocyanide Ylides

Javier E. Alfonso-Ramos,[a] Ruben Van Lommel*,[b,c] David Hernández-Castillo,[a] Frank De Proft,[c] Roy González-Alemán,[a] Erik V. Van der Eycken[d,e] and Gerardo M. Ojeda-Carralero*[d,f]

[a] J.E. Alfonso-Ramos., R. González-Alemán, D. Hernández-Castillo.
Laboratory of Computational and Theoretical Chemistry (LQCT)
Faculty of Chemistry, University of Havana
Zapata y G, 10400 Havana, Cuba
[b] R. Van Lommel
Molecular Design and Synthesis
Department of Chemistry, KU Leuven
Celestijnenlaan 200F Leuven Chem&Tech, box 2404, 3001 Leuven, Belgium
E-mail: ruben.vanlommel@kuleuven.be
[c] R. Van Lommel, Prof. F. De Proft
Eenheid Algemene Chemie (ALGC)
Department of Chemistry, Vrije Universiteit Brussel (VUB)
Pleinlaan 2, 1050 Brussels, Belgium
[d] G. M. Ojeda-Carralero, Prof. E. V. Van der Eycken
Laboratory for Organic & Microwave-Assisted Chemistry (LOMAC)
Department of Chemistry, KU Leuven
Celestijnenlaan 200F Leuven Chem&Tech, box 2404, 3001 Leuven, Belgium
[e] Prof. E. V. Van der Eycken
Peoples' Friendship University of Russia (RUDN University)
Miklukho-Maklaya Street 6, 117198 Moscow, Russia
[f] G. M. Ojeda-Carralero
Department of General and Inorganic Chemistry, Faculty of Chemistry
University of Havana, Zapata y G, 10400 Havana, Cuba
E-mail: gmojedac@gmail.com

Supporting information for this article is given via a link at the end of the document.

Abstract: 1,3-dipolar cycloadditions are the preferred method to generate five-membered heterocyclic rings. Surprisingly, cycloadditions based on acyl-isocyanide ylides have remained underexplored by the chemical community. Acyl-isocyanide ylides readily react with dipolarophiles, such as substituted alkenes, to yield Δ^1-pyrroline derivatives. As an explanation for the observed reactivity of this reaction is lacking, extensive density functional theory calculations were performed to scrutinize the mechanistic features of the transformation. Herein we explain the experimental outcome of the reaction using a variety of reactivity theories and predict opposed regioselectivity for electron-poor and electron-rich dipolarophiles. With the insights obtained, we hope to incentivize the design of new cycloaddition reactions based on the acyl-isocyanide ylides motif.

Introduction

Cycloaddition reactions remain an active research field for experimental and theoretical chemists alike. Indeed, these procedures are receiving great interest because of their inherent complete atom economy, and the high yields and chemo-, regio- and stereoselectivity they can display. One type of cycloaddition, the so-called Huisgen reaction (Scheme 1a) involving the (3+2) cycloaddition of 1,3-dipoles to multiple-bond systems (dipolarophiles), has become a principal method for the construction of five-membered heterocycles.[1] The continued discovery of new reactivity based on dipoles and dipolarophiles has evolved into many powerful synthetic methods.[2] For example, the copper(I)- or ruthenium(II)-catalyzed azido alkyne cycloaddition (CuAAC and RuAAC, respectively) and their strain-promoted versions to form disubstituted triazoles have developed into the cornerstone of Click chemistry and bioorthogonal chemical ligation (Scheme 1b).[3] Additionally, dipolar cycloaddition procedures are paramount for the (semi)synthesis of drug candidates and next-generation materials.[4]

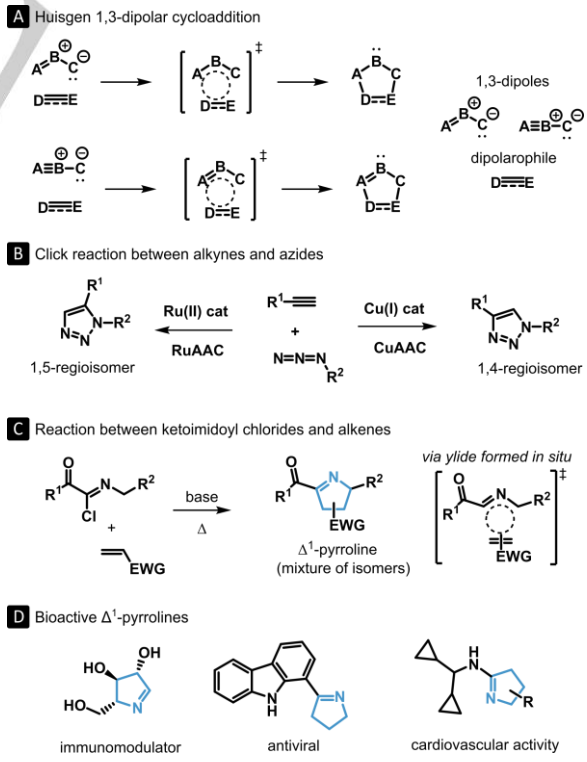

Scheme 1. Cycloadditions of 1,3-dipoles to dipolarophiles. EWG = electron withdrawing group.

In parallel, isocyanide-based chemistry has experienced a tremendous growth during the last decades.[5] The unique properties of the isocyanide (also known as isonitrile) moiety allows its reaction with nucleophiles, electrophiles, acids, bases, free radicals and metal centers. Not surprisingly, there have been several efforts to merge isocyanide and dipolar cycloaddition chemistry, giving rise to different catalytic and tandem processes.[6] In this context, Livinghouse and Tian were the first to report the reaction between α-ketoimidoyl chlorides and methyl acrylate in the presence of suitable (non-nucleophilic) organic bases such as DBU (Scheme 1c).[7] In their work, they hypothesize that the reaction involves acyl-isocyanide ylides as reactive intermediates in a 1,3-dipolar cycloaddition fashion. Later, the same reaction was reported for *exo* and *endo* α,β-unsaturated lactones.[8] The procedure renders the corresponding Δ^1-pyrrolines in a moderate yield and regioselectivity. Δ^1-pyrrolines are heterocyclic moieties found in biologically relevant compounds and metabolic intermediates; moreover, they can be useful synthetic intermediates amenable for further functionalization (Scheme 1d).[9] To our surprise, this reaction has largely been overlooked by the organic chemistry community, and to the best of our knowledge there has been no attempt to elucidate its reactivity other than the present work.

Over the years, much effort has been devoted into explaining the mode of action of many 1,3-dipolar cycloaddition reactions, and to make predictions of their experimental outcome.[10] To accomplish this, frontier molecular orbital analysis,[11] Fukui reactivity indices[12] and the distortion/interaction-activation/strain (DIAS) model and energy decomposition analysis (EDA)[13, 14] have, among others, served as practical frameworks for the study of these transformations.[13-15] Recent examples include the elucidation of the catalytic effects of a Lewis base, as well as unravel the factors controlling the (a)synchronicity and concerted character of the bond formations.[16] Herein, the reactions between numerous substituted alkenes and acyl-isocyanide ylides were computationally investigated through DFT based methods, including the quantification of the activation barrier, frontier molecular orbital analysis and the DIAS/EDA scheme, in an attempt to explain the intricacies of this long-forgotten reaction.

Computational Details

Gaussview[17] was used to create all structures, while geometry optimization and frequency analysis of reactants, products and transition state structures were performed at the M06-2X/6-311+G(d) level of theory[18] using Gaussian 16 (version A.03)[19] with the integration grid set to ultrafine.[20] Acetonitrile solvation effects on the geometries of the structures were accounted for through the SMD implicit solvent model.[21] Importantly, the selected M06-2X exchange-correlation functional already showed to produce reasonable activation enthalpies for 1,3-dipolar cycloaddition reactions.[22] The structures of all reactants, products and prereactive complexes were characterized exclusively by positive eigenvalues of the Hessian matrix, while transition state structures were characterized by a single negative eigenvalue. Intrinsic Reaction Coordinate (IRC) analysis confirmed the transition state to correctly connect the reactant state to the corresponding product. Subsequent gas phase single point energies were calculated at the M06-2X/TZ2P level of theory[23] using the ADF2019 software[24] in combination with the open-source PyFrag module (version 2019)[25] to streamline the distortion/interaction-activation/strain model and energy decomposition analyses. The density fitting quality and numerical integration quality were set to very good. Comparison of activation energies showed that changing the basis set from 6-311+G(d) to TZ2P had a negligible effect on the results obtained (see Figure S5 in the supporting information).

Non-covalent Interactions (NCI) analyses were based on the M06-2X/6-311+G(d) generated wavefunction and were performed using the NCIPLOT software (version 4.0).[26, 27] Finally, CYLview20 and VMD were used to visualize results and create images of the structures.[28] Coordinates of the stationary points are provided in the supporting information (section 5) and were generated with assistance of the ESIgen code.[29].

Results and Discussion

Regioselective considerations

Nitrile ylides have enjoyed the attention of the synthetic organic chemistry community due to their potency to undergo dipolar cycloadditions. However, the use of ylides derived from isocyanides remains underexplored. Particularly the acyl-isocyanide ylides, which are *in situ* generated from the treatment of α-ketoimidoyl chlorides with mild bases, can be of interest. Indeed, the α-ketoimidoyl chlorides, which serve as one of the reactants in this transformation, can be easily prepared by direct interaction between isocyanides and acyl chlorides, in the so-called Nef reaction.[30] Although α-ketoimidoyl chlorides show a high reactivity towards inter- and intramolecular nucleophilic functionalities, it was found that they can be trapped by suitable dipolarophiles such as acrylates and trifluoroacetophenone.[7, 31] The reaction yields a complex isomeric mixture influenced by the regioselective preference. Moreover, the transformation can either proceed through an *endo*- or *exo* pathway, ultimately influencing the stereoselectivity of the formed products as well. Focussing on the regioselectivity, it is clear from experimental results that the relative regioisomeric ratio between the products is dependent on the substrates used (Table 1, reactions **1**-**5**). It was found that the reactions generally favour the formation of isomer **I**, in which the R^2 and R^3 substituents from the dipole and the dipolarophile, respectively, are in the nearest proximity to each other. Notably, when the reaction was performed using trifluoroacetophenone as dipolarophile, only a slight amount of isomer **II** could be recovered (reaction **5**).[7].

So far, the experimental studies of the reaction between acyl-isocyanide ylides are limited to acrylate or the related α,β-unsaturated lactone dipolarophiles.[8] Therefore, the electronic requirements of the reaction remains obscure. We intended to understand the key factors controlling the reactivity and investigate other model alkene dipolarophiles (*i.e.,* bearing a substituent other than the ester group, Table 1 entries **6-9**). In addition, we investigated the reaction with ethene as reference point for our discussion (Table 1, entry **10**). With that, we studied a total of 10 reactions between acyl-isocyanide ylides and trifluoroacetophenone or alkene-based dipolarophiles (Table 1).

10.1002/ejoc.202201028

Table 1. Reactions considered in this study. The experimental yields found by Livinghouse and Tian (entries **1**-**5**) are shown.[7]

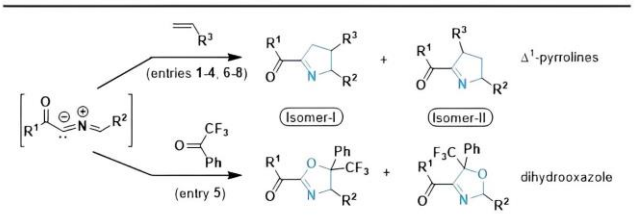

entry	1,3-dipole		dipolarophile	Yields		
	R^1	R^2		I	II	I/II ratio
1	*tert*-butyl	H		46	17	2.70
2	*iso*-propyl	H	methyl	64	10	6.40
3	cyclopropyl	H	acrylate	55	11	5.00
4	*tert*-butyl	Ph		49	13	3.77
5	*tert*-butyl	H	trifluoromethyl-phenylketone	43	3	14.30
			Model reactions			
6	*tert*-butyl	H	nitroethene	-	-	-
7	*tert*-butyl	H	cyanoethene	-	-	-
8	*tert*-butyl	H	propene	-	-	-
9	*tert*-butyl	H	methoxyethene	-	-	-
10	*tert*-butyl	H	ethene	-	-	-

Mechanistic elucidation and frontier molecular orbitals

To understand the mechanistic aspects and charge transfer occurring during the transformation, we first analysed the frontier molecular orbitals (FMOs) of the reactants (see Figure S1 in the supporting information). By quantifying the energy gaps between the FMOs of the dipole and the dipolarophile (and considering the orbital symmetries and correct geometries to enable overlap of the orbitals) one can obtain information on the origin of the primary orbital interactions that occur during the reaction.[13, 32] For 1,3-dipolar cycloadditions, three situations can unfold. If the orbital interaction mainly originates from overlap of the HOMO of the dipole ($HOMO_D$) with the LUMO of the dipolarophile ($LUMO_{DA}$), the reaction is classified as a type I, normal electron demand (NED) cycloaddition (Table 2, $\varepsilon_1 < \varepsilon_2$). Alternatively, the orbital interaction can mainly stem from overlap between the HOMO of the dipolarophile ($HOMO_{DA}$) and the LUMO of the dipole ($LUMO_D$), and in this case the cycloaddition follows a type III, inverse electron demand (IED) pathway (Table 2, $\varepsilon_1 > \varepsilon_2$).[1, 32] Finally, an intermediate type II case exists, for which a double pairwise orbital interaction between $HOMO_D$ and $LUMO_{DA}$ and between $HOMO_{DA}$ and $LUMO_D$ occurs (Table 2, $\varepsilon_1 \approx \varepsilon_2$). Taking note of the energy gaps between the overlapping frontier molecular orbitals of the acyl-isocyanide ylide dipoles and dipolarophiles, it can be discerned that reactions **1**-**7** and reference reaction **10** proceed through an NED dipolar cycloaddition ($\varepsilon_1 < \varepsilon_2$). In contrast, **8** proceeds *via* a type II dipolar cycloaddition ($\varepsilon_1 \approx \varepsilon_2$), while **9** follows an IED dipolar cycloaddition ($\varepsilon_1 > \varepsilon_2$). These observations can be explained by the substituent present on the dipolarophile. Indeed, for reactions **1**-**7** the dipolarophiles used are all electron-poor carbonyl derivatives or alkenes bearing an electron withdrawing group ($-CF_3$; R^3 = $-COOCH_3$, $-NO_2$, $-CN$; respectively). In reaction **10**, on the other hand, the dipolarophile is ethane which bears no substituents. Although this leads to a decrease in the gap between ε_1 and ε_2 ($\Delta\varepsilon_{2\text{-}1}$, Table 2), the relative levels of the FMOs still results in an NED pathway for **10**. Finally, reactions **8** and **9** make use of alkenes that have an electron donating group (R^3 = $-CH_3$, $-OCH_3$), giving rise to an electron-rich double bond. These electron donating groups cause an increase of the energy levels of the HOMO and LUMO of the dipolarophile, resulting in a shift from type I to type II and ultimately to type III cycloaddition. Moreover, based on these results, and corroborated by the difference in chemical potential of the dipole and dipolarophile (see Table S1 in the supporting information), it is clear that the electron flow goes from dipole to dipolarophile during reactions **1**-**7** and **10** and from dipolarophile to dipole for **9**. For **8**, a negligible charge transfer between the reactants is expected.

Table 2. Energy gaps between the frontier orbitals of the dipole and dipolarophile for entries **1-10**. Frontier orbitals of the starting materials of reaction **1** are shown.

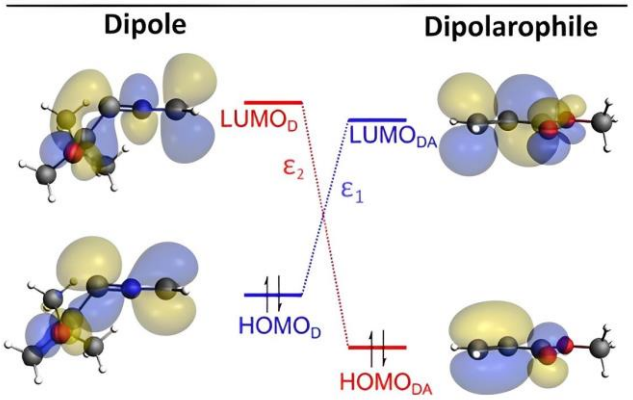

entry	ε_1 ($LUMO_{DA}$-$HOMO_D$) (eV)	ε_2 ($LUMO_D$-$HOMO_{DA}$) (eV)	$\Delta\varepsilon_{2\text{-}1}$ (eV)	Electron demand
1	6.923	9.499	2.576	NED
2	6.990	9.453	2.463	NED
3	6.987	9.451	2.464	NED
4	7.981	8.676	0.758	NED
5	5.774	9.111	3.337	NED
6	5.665	10.531	4.866	NED
7	6.600	9.652	3.052	NED
8	8.674	8.545	-0.129	type II
9	8.782	7.762	-1.020	IED
10	8.372	9.092	0.720	NED

Kinetic considerations and transition states

To obtain a better understanding of the mode of action of the reactions, we located the transition states for the concerted formation of regioisomers **I** ($TS_{X\text{-}I}$) and **II** ($TS_{X\text{-}II}$) and considered both the *endo*- and *exo* pathways to reach these regioisomers (see section 5 in the supporting information). For reaction **4** we additionally considered the formation of the *cis* and *trans* isomers and selected the path with the lowest calculated activation energy for further analysis. The transition states were found for all reactions and pathways, with the exception of $TS_{4\text{-}II\text{-}endo}$ and $TS_{5\text{-}II\text{-}endo}$ (Figure 1). We hypothesize that our inability to locate these transition states stems from the steric congestion between the reactants in the *endo* conformation. The transition states for **1**-**4**, **6** and **7** share common structural features (Figure 1a+b). Indeed, transition states giving rise to isomer **I** ($TS_{X\text{-}I\text{-}endo}$ and $TS_{X\text{-}I\text{-}exo}$) show a high degree of asynchronicity, as expressed by the

absolute difference in C–C bond lengths observed in the transition state structure ($\Delta r_{C\cdots C}$). Bond formation between the secondary C of the dipole ylide and the terminal C of the alkene dipolarophile precedes bond formation between the terminal C of the dipole and the secondary C of the dipolarophile. Moreover, the degree of asynchronicity in these transition states increases in parallel with the electron withdrawing ability of the substituent in the alkene, being the largest for **6** (–NO_2). In contrast, the corresponding transition states giving rise to isomer **II** ($TS_{X\text{-}II\text{-}endo}$ and $TS_{X\text{-}II\text{-}exo}$) are nearly synchronous (Figure 1c+d). The opposite is observed for reaction **5**, in which the most asynchronous transition state corresponds to the formation of **II** ($TS_{5\text{-}II\text{-}exo}$). On the other hand, the transition states for reactions **8**,**9** and **10** are all characterized by a high synchronicity, independent on the regioselectivity and despite the difference in electron donating properties of the substituent on the dipolarophile (–CH_3 vs. –OCH_3 vs. –H, respectively).

With the transition state structures of the reactions yielding the different regioisomers in hand, we could obtain the associated activation barriers (ΔE_a) (Table 3). The latter is computed by subtracting the electronic energy of the isolated reactants from the transition state. Focussing exclusively on the pathway with the lowest activation barriers, we found that the activation barriers yielding isomer **I** were lower compared to the barriers giving rise to **II** for reactions **1**-**4**, in agreement with the reported experimental data from Livinghouse and Tian.[7] A similar trend is observed for model reactions **6**-**7**, suggesting that these reactions would favour the formation of **I** over **II** as well. Moreover, for reaction **4**, our calculations showed a preference towards the formation of the *cis* and *trans* product, for regioisomer **I** and **II**, respectively. This finding is again in line with experimental results.[7] For **1**-**7** the reaction proceeds preferentially through an *exo* pathway. Reactions **8** and **9**, on the other hand, preferentially proceed through an *endo* pathway and are characterized by a lower barrier for **II** (9.5 and 8.8 kcal.mol^{-1}, respectively) compared to **I** (10.1 and 11.1 kcal.mol^{-1}, respectively). Moreover, both **8**, **9** and **10** have a significantly higher activation barriers for the cycloaddition, being as much as 10 kcal·mol^{-1} higher than the activation barriers calculated for **1**-**7**. Looking at the activation barriers computed for **5**, it could be discerned that the formation of **II** is preferred over regioisomer **I**, which disagrees with the experimental results obtained by Livinghouse and Tian.[7] Notably, when the barrier of the reaction accounts for the stability of the pre-reactive complex, *i.e.* ΔE_a^{pre} is calculated by subtracting the energy of the pre-reactive complex to the transition state, the experimental regioselectivity is retrieved from the computations (Table 3). In addition, the same regioselectivity preferences can be predicted based on the condensed Fukui functions of the reactants in all cases (see section 2.2 in the supporting information) and the computed regioselective preference seems to be correlated to the charge transfer pathway between the reactive species, *i.e.* NED, type II or IED, (Table 2).

To elucidate the factors determining the height of the activation barrier, the DIAS model (also known as activation strain model (ASM) in the literature) and EDA are applied to the potential energy surface of the reaction in the gas phase.[13, 14] The fragment-based DIAS model decomposes the total electronic energy (ΔE) into a strain term (ΔE_{strain}) that considers the distortion penalty associated with deforming the reactants into the transition state complex and an interaction term (ΔE_{int}) that values the mutual interactions between them [Eq. (1)]. In turn, the strain energy can be further fragmented to evaluate the contribution of the different reactants towards the total strain [Eq. (2)]. The EDA on the other hand, decomposes the interaction energy into a Pauli repulsion (ΔE_{Pauli}), orbital interaction (ΔE_{oi}) and electrostatic interactions (ΔV_{elstat}) [Eq. (3)]. Table 3 shows the results of the DIAS and EDA applied on the transition state structures, using the values associated with the optimized reactants as the baseline.

$$\Delta E(\xi) = \Delta E_{\text{strain}}(\xi) + \Delta E_{\text{int}}(\xi) \quad (\mathbf{1})$$

$$\Delta E_{\text{strain}}(\xi) = \Delta E_{\text{strain}}^{\text{dipole}}(\xi) + \Delta E_{\text{strain}}^{\text{dipolarophile}}(\xi) \quad (\mathbf{2})$$

$$\Delta E_{int}(\xi) = \Delta E_{\text{Pauli}}(\xi) + \Delta E_{\text{oi}}(\xi) + \Delta V_{\text{elstat}}(\xi) \quad (\mathbf{3})$$

10.1002/ejoc.202201028

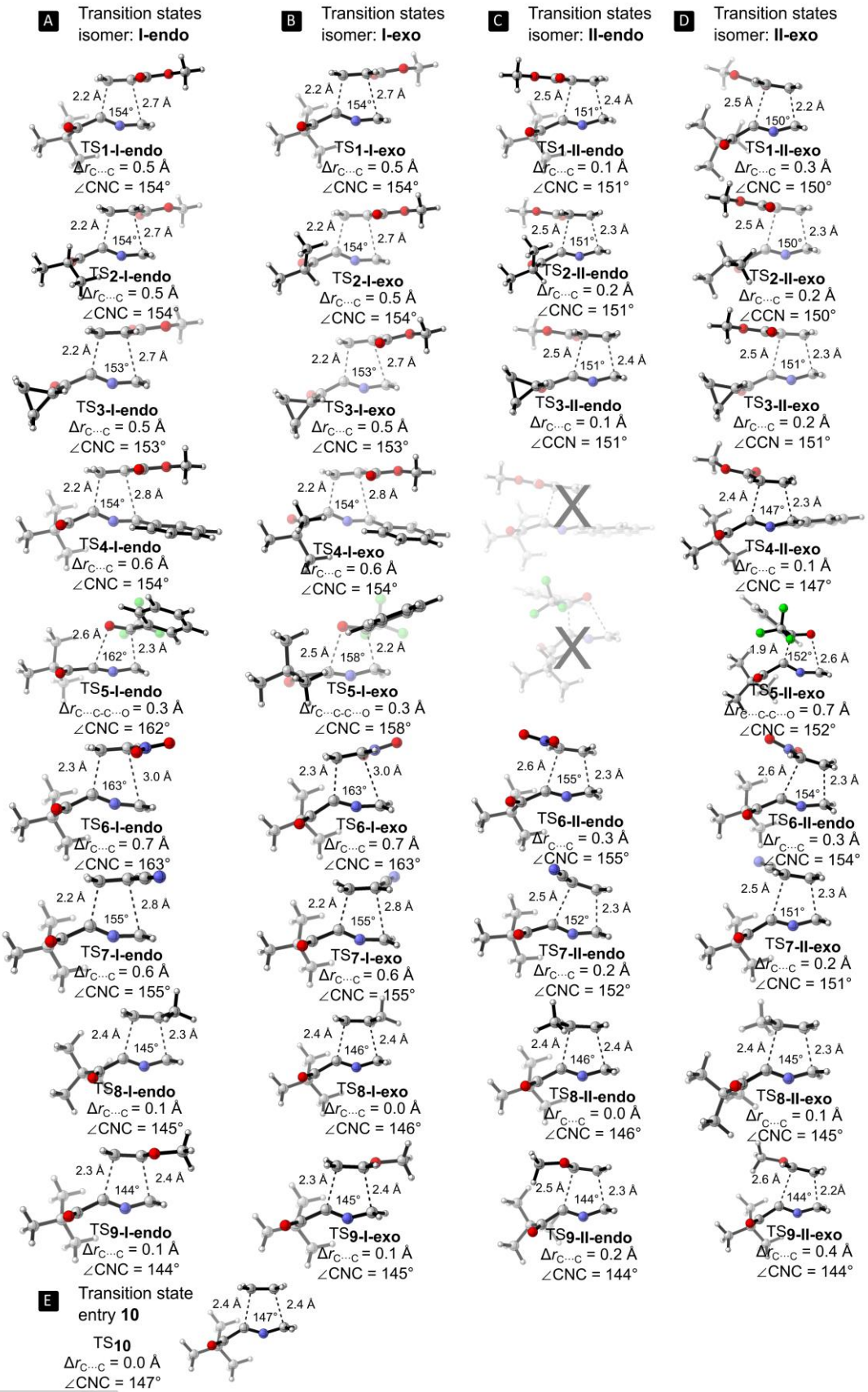

Figure 1. Transition states for **1**-**9** resulting in regioisomer **I** through the **a)** *endo* or **b)** *exo* pathway or regioisomer **II** through the **c)** *endo* or **d)** *exo* pathway. **e)** Transition state for **10**. Below the structures, the values of the difference in bond distances ($\Delta r_{C\cdots C}$) and ∠CNC is provided. TS are labeled in *endo* or *exo* conformations according to the carbonyl if the ylide and the alkene substituent lay in same or different face of the pyrroline ring, respectively. Optimized geometries are obtained at the M06-2X/6-311+g(d) level of theory, with acetonitrile solvation effects included using the SMD implicit solvent model.

Table 3. The distortion/interaction-activation/strain model and energy decomposition analysis of the transition states of reactions **1-10** giving rise to either isomer **I** or isomer **II** *via* an *endo* or *exo* pathway. For reaction **4** only the data for the preferred *cis*/*trans* isomer is shown. Results are obtained at the M06-2X/TZ2P//M06-2X/6-311+g(d) level of theory (geometry optimization included solvation effects through SMD=acetonitrile) and expressed in kcal.mol^{-1}. ΔE_a is calculated as the difference between the energy of the transition state and the isolated reactants, and the DIAS analysis is referred to this quantity. ΔE_a^{pre} is calculated as the difference between the energy of the transition state and the pre-reactive complex. The lowest value of ΔE_a for each reaction is labelled in bold.

entry-isomer	ΔE_a	ΔE_a^{pre}	ΔE_{strain}	$\Delta E_{\text{strain}}^{\text{dipole}}$	$\Delta E_{\text{strain}}^{\text{dipolarophile}}$	ΔE_{int}	ΔE_{Pauli}	ΔE_{oi}	ΔV_{elstat}
1-I-endo	3.0	6.3	11.3	7.1	4.2	-8.3	59.2	-33.1	-34.4
1-II-endo	2.5	7.0	13.6	10.6	3.1	-11.2	50.3	-29.4	-32.0
1-I-exo	**1.4**	6.2	14.0	8.8	5.3	-12.6	66.1	-39.1	-39.6
1-II-exo	2.2	8.0	15.1	10.7	4.4	-12.9	56.9	-34.6	-35.2
2-I-endo	3.5	6.6	11.5	7.3	4.2	-8.0	59.2	-32.9	-34.3
2-II-endo	3.0	7.2	13.9	10.7	3.2	-10.9	49.8	-29.4	-31.3
2-I-exo	**1.6**	5.9	11.3	7.3	4.0	-9.7	57.3	-32.3	-34.8
2-II-exo	1.8	7.4	14.3	10.7	3.6	-12.5	52.6	-31.8	-33.2
3-I-endo	3.5	6.3	11.6	7.4	4.1	-8.1	58.9	-32.8	-34.1
3-II-endo	3.6	7.1	14.1	11.0	3.0	-10.5	49.9	-29.1	-31.4
3-I-exo	**2.4**	6.4	14.4	9.1	5.3	-12.0	66.6	-39.2	-39.4
3-II-exo	2.4	7.1	13.8	10.6	3.2	-11.3	50.5	-30.0	-31.9
4-I-endo (cis)	0.5	6.8	11.0	6.4	4.6	-10.5	64.7	-36.4	-38.8
4-II-endo (?)									
4-I-exo (trans)	**-1.5**	5.6	10.2	6.0	4.2	-11.7	60.7	-34.5	-37.9
4-II-exo (trans)	3.3	9.1	16.7	12.5	4.2	-13.4	56.7	-34.3	-35.8
5-I-endo	3.2	6.5	19.5	9.2	10.3	-16.3	50.8	-33.9	-33.3
5-II-endo									
5-I-exo	4.6	6.9	23.3	12.1	11.2	-18.7	69.5	-46.4	-41.8
5-II-exo	**3.0**	9.7	28.1	8.9	19.2	-25.1	131.8	-82.3	-74.7
6-I-endo	-0.1	4.2	6.1	2.2	3.9	-6.2	45.4	-24.6	-27.0
6-II-endo	2.3	5.8	11.9	8.0	3.8	-9.6	45.8	-28.1	-27.2
6-I-exo	**-2.1**	4.4	6.4	2.2	4.2	-8.5	46.6	-25.9	-29.2
6-II-exo	-0.5	6.0	12.4	8.0	4.5	-12.9	49.3	-30.8	-31.4
7-I-endo	3.1	6.8	10.4	6.0	4.4	-7.3	63.8	-34.5	-36.6
7-II-endo	5.4	7.4	13.4	9.7	3.7	-8.1	50.8	-30.2	-28.7
7-I-exo	**2.2**	7.0	10.3	6.0	4.3	-8.1	63.0	-34.2	-36.9
7-II-exo	3.2	7.4	14.3	9.9	4.4	-11.1	53.7	-32.5	-32.3
8-I-endo	10.3	12.5	19.3	13.8	5.6	-9.0	56.2	-31.5	-33.7
8-II-endo	**9.5**	11.4	18.5	13.6	5.0	-9.1	54.4	-29.9	-33.5
8-I-exo	10.1	12.0	19.1	13.7	5.5	-9.0	54.7	-30.8	-32.9
8-II-exo	10.5	12.8	19.9	14.4	5.5	-9.4	57.3	-32.3	-34.5
9-I-endo	11.8	13.4	21.0	15.4	5.6	-9.2	59.9	-33.9	-35.2
9-II-endo	**8.8**	12.4	19.8	15.2	4.6	-11.1	57.6	-32.8	-36.0
9-I-exo	11.1	13.3	20.9	15.3	5.6	-9.8	59.7	-33.8	-35.7
9-II-exo	9.4	13.3	21.0	16.2	4.8	-11.6	60.1	-34.4	-37.3
10	7.5	9.3	15.8	12.3	3.5	-8.3	51.4	-29.1	-30.7

The results of the DIAS analysis at the transition state reveals the importance of the strain contribution towards the total activation barrier. Indeed, while one might hypothesize that the increased activation barrier of **8**, **9** and **10** is explained by the absence of electrostatic effects exerted by an electron withdrawing group on the dipolarophile (which is present for **1**-**7**), it is in fact the increased strain penalty of the transition state relative to the isolated reactants that causes the observed increase. Deeper analysis of the strain term indicates that for **1**-**4** and **6**-**10**, the majority of the strain in the transition state originates from the isocyanide-derived ylide dipole. Analysis of the ∠CNC dipole angle clearly shows that for these reactions the transition state requires a significant distortion from the linear ∠CNC of the reactant (Figure 1). Intriguingly, analysis of the strain terms on the transition states of **5** reveals that in this exceptional case both the dipole and dipolarophile contribute almost equally. Moreover, the terms resulting from the EDA are substantially different for isomer **I** and **II** in reaction **5** (Table 3). This is especially striking in comparison to the differences in the terms of the EDA between **I** and **II** observed for the other reactions. This merits a closer analysis of the non-covalent interactions present in the transition states of reaction **5**.

Non-covalent interactions in the transition state complex

By performing an NCI analysis on a transition state structure, one can observe the non-covalent interactions between the reactants in the activated complex.[33] Herein, we used the NCI analysis on the *exo* transition states of **5** resulting in isomer **I** ($TS_{\textbf{5-I-}exo}$) or **II** ($TS_{\textbf{5-II-}exo}$), in an attempt to gain a better understanding behind the substantial differences in the interactions between these regioselective reactions. Indeed, the EDA quantified a significant difference in the interaction terms between both reactions (Table 3). Through the reduced density gradient (*s*) isosurfaces present in $TS_{\textbf{5-I-}exo}$ and $TS_{\textbf{5-II-}exo}$, the non-covalent interactions are visualized. Notably, the orientation of the *tert*-butyl group of the dipole with respect to the phenyl-substituent of the dipolarophile allows for weakly stabilizing CH···π interactions during formation of **II** *via* $TS_{\textbf{5-II-}exo}$. Recalling the resulting EDA of this reaction in Table 3, we can conclude that the collection of these stabilizing interactions (which consists of both electrostatics and orbital interactions) overcomes the large sterical hindrance (Pauli repulsion), the latter being influenced by the proximity of the bulky *tert*-butyl group to the dipole. The aforementioned CH···π interactions are not possible during the reaction towards **I** *via* $TS_{\textbf{5-I-}exo}$ as the *tert*-butyl group is positioned away from the phenyl-substituent. Instead, a weak stabilizing non-covalent interaction between the aryl hydrogen and the *tert*-butyl group is observable (Figure 2a). These non-covalent interactions also appear in the 2-dimensional plot of *s* as characteristic troughs (Figure 2b). In this plot, the positioning of some of the troughs, which is indicative of the nature of the non-covalent interaction ($\rho \cdot \text{sign}(\lambda_2) > 0$ = repulsive, $\rho \cdot \text{sign}(\lambda_2) < 0$ = attractive) are notably different. These

10.1002/ejoc.202201028

differences form an important contribution towards the interaction between the reactants. However, we do take note that these interactions are also accompanied by an extensive deformation of the dipolarophile, which is best described by the deviation of the ∠$C_{ortho}C_{ipso}CO$ torsion away from the ideal *anti*-conformation (-149.39 ° in $TS_{5\text{-}I\text{-}exo}$ and -131.04 ° in $TS_{5\text{-}II\text{-}exo}$). The latter explains why **5** is an exceptional case for which also the dipolarophile contributes significantly towards the total strain penalty of the reaction (Table 3).

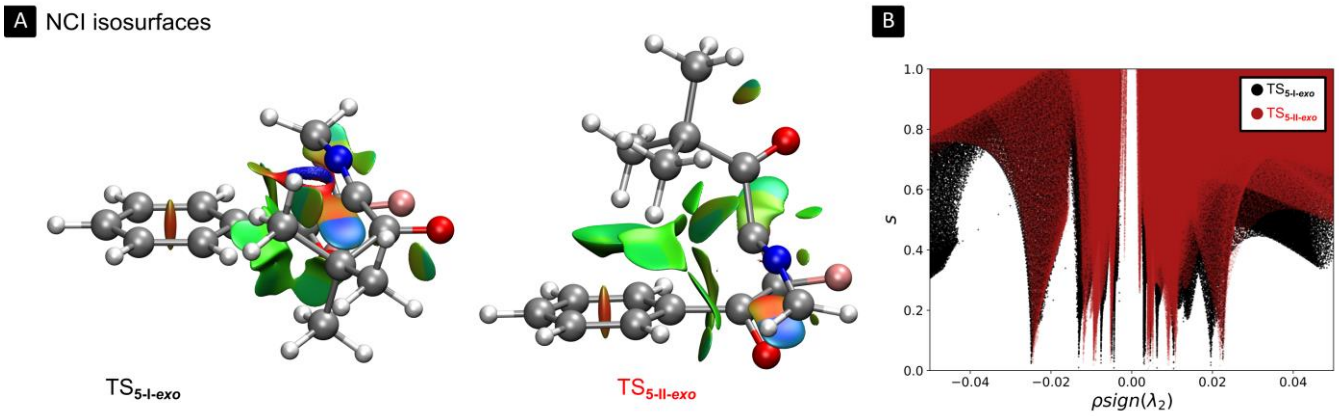

Figure 2. a) Visualization of the 3-dimensional NCI isosurfaces (*s* = 0.5) for the transition states of entry **5** resulting in isomer **I** (left, black) or **II** (middle, red) through the *exo* pathway. An RGB colour scale set from -0.003 a.u. to 0.003 a.u. is used to differentiate between repulsive (red), weak (green) and attractive (blue) non-covalent interactions. **b)** Accompanying overlay plot of the reduced density gradient *s* in function of ρ·sign(λ_2).

Generalizing the influence of the dipolarophile's substituent

In order to arrive at a more general picture of the studied reactions, we decided to search for quantitative relations between the computed properties of the *exo* reactions towards isomer **I** ($\varepsilon_{1/2}$, ΔE_a, E_{strain} …) and the electronics of the dipolarophile's substituent. In this analysis, we focused on reactions **1** and **6**-**10**, in which the dipole remains the same. In this manner we single out effects caused by variation of the substituent on the alkene dipolarophile. Because the substituents of interest are directly attached (and conjugated) to the double bond, we decided to describe their electron withdrawing- or donating power using the Hammett σ_p parameter.[34] Hammett parameters have found widespread utility when studying reaction mechanisms and are useful for explaining trends in molecular reactivity, with emphasis on aromatic compounds.[34,35] Strong electron-withdrawing groups (EWG) have high (positive) values of σ_p, meaning that electron density flows away from the conjugated system; while strong electron-donating groups (EDG) have low (negative) values of σ_p, meaning that electron density flows towards the conjugated system. In this study, the dipolarophiles will have an electron rich or poor double bond when bearing substituents with negative or positive values of σ_p, respectively.

Striking correlations between the calculated properties of the reactions and the σ_p parameters were retrieved. Indeed, decreasing the σ_p of the substituent leads to an increase of ε_1 and a decrease of ε_2 (Figure 3a, see Table S3 in the supporting information). This can be explained by a simultaneous increase of the energy level of the HOMO and the LUMO frontier molecular orbitals of the dipolarophile upon decreasing σ_p. Therefore, there is a transition from an NED (**1**, **6**, **7** and **10**) to a type II (**8**) and ultimately an IED (**9**) 1,3-dipolar cycloaddition when increasing the electron donating properties of the substituent on the dipolarophile. Figure 3b also illustrates that decreasing σ_p causes an increase in the activation energy. The DIAS and EDA concluded that all the analyzed reactions of **1** and **6**-**10** proceed with a similar interaction energy and a comparable dipolarophile strain penalty (Table 3). Hence, the overall increase in ΔE_a is better explained by the continued increase of the strain of the 1,3-dipole, that shows a similar trend as the total strain penalty as well as the activation barrier upon varying σ_p (Figure 3b).

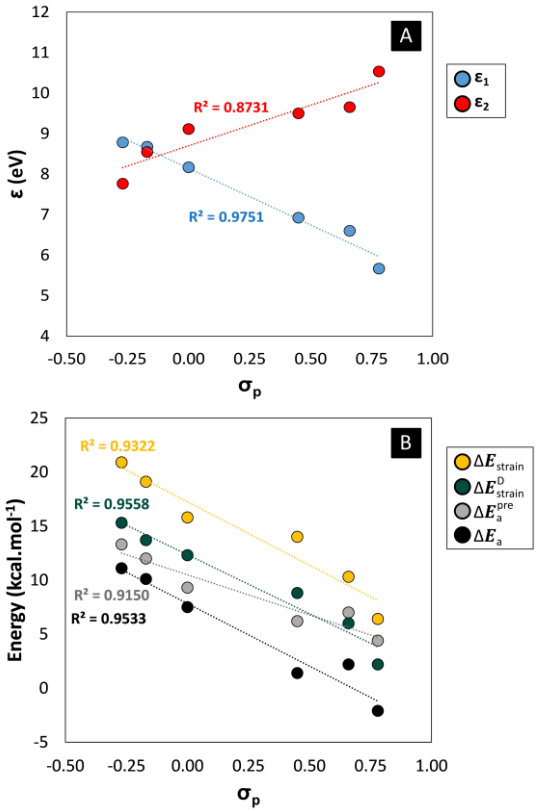

Figure 3. a) Linear correlations between HOMO-LUMO gaps (ε_1 (blue) and ε_2 (red)) and Hammet parameter σ_p of the dipolarophile's substituent. **b)** Linear correlations between energetic properties of the reaction and the Hammet parameter σ_p of the dipolarophile's substituent. Data stems from reaction **1** and **6**-**10** and considers the *exo* pathway towards isomer **I**.

10.1002/ejoc.202201028

What is the underlying factor explaining this trend? Further analyses revealed the importance of both the variation of the ∠CNC angles and the r(N-C5) bond distance of the acyl-isocyanide ylide fragments in the transition states to explain the origin of the strain. Electron poor dipolarophiles tend to undergo an asynchronous reaction (Figure 1 and Figure 4a). In the corresponding transition state, the ylide HOMO, largely located on the C2 atom, donates electronic density to the alkene LUMO. As a result, the N-C5 bond remains essentially unaltered as a double bond, *i.e.* N has more sp character and ∠CNC is closer to the value of the optimized reactant (176.1º) (Figures 4b). In contrast, electron rich alkenes (those bearing substituents with a negative σ_p) tend to undergo reactions with a higher synchronicity. In the corresponding transition state, the alkene HOMO donates electronic density to the dipole's LUMO, largely located on the C5 atom. As result, the N-C5 bond is considerable weakened, *i.e* the N has more sp^2 character, the ∠CNC is considerably distorted and the dipole fragment is more bent.

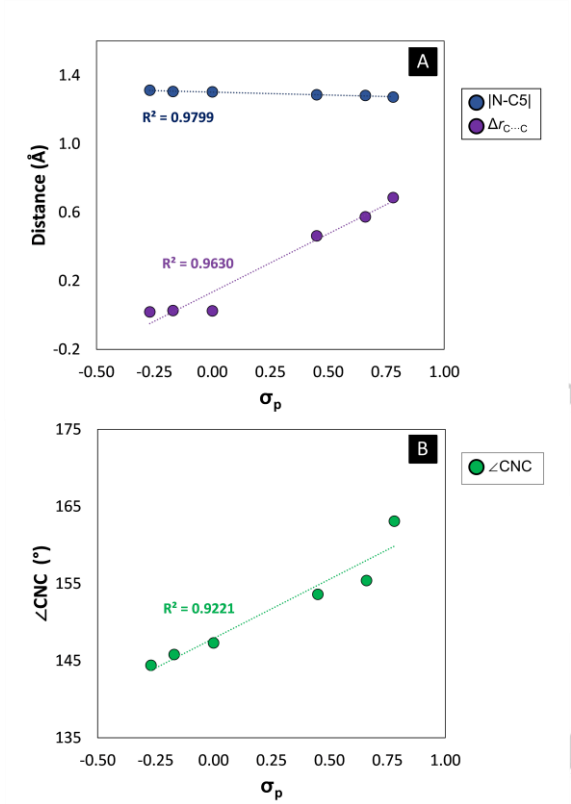

Figure 4. a) Linear correlations between |N-C5| bond distance and difference in bond distances ($\Delta r_{C\cdots C}$) with the Hammet parameter σ_p of the dipolarophile's substituent. **b)** Linear correlations between ∠CNC and the Hammet parameter σ_p of the dipolarophile's substituent. Data stems from reaction **1** and **6**-**10** and considers the *exo* pathway towards isomer **I**.

Conclusion

The preparation of Δ^1-pyrrolines through a 1,3-dipolar cycloaddition reaction of acyl-isocyanide ylides with a dipolarophile has received limited attention so far. In this work, we used density functional theory-based methods to elucidate the reactivity driving this transformation. Analysis of the frontier molecular orbitals showed that the reaction can proceed both through a normal electron demand, a type II cycloaddition, or an inverse electron demand pathway, depending on the electron withdrawing (NED) or donating (IED) properties of the substituent on the dipolarophile.

Furthermore, by linking the structural and energetic properties of the transition states with the electronics of the dipolarophile, two general scenarios for the mechanism of the 1,3-dipolar cycloaddition reaction between acyl-isocyanide ylides and alkenes are plausible (Figure 5). **Case A**; reactions comprising electron deficient dipolarophiles (*i.e.* alkenes bearing an electron withdrawing group) proceed at relatively lower activation energies *via* asynchronous bond formation, with preference towards isomer **I** *via* an *exo* pathway. These are type I (NED) dipolar cycloadditions in which the electron density flows from the dipole towards the dipolarophile. The activation energy is low due to a minimum distortion of the dipole in the transition state. **Case B**; reactions comprising electron rich dipolarophiles (*i.e.* alkenes bearing an electron donating group) proceed at relatively higher activation energies *via* synchronous bond formation, with preference towards isomer **II**. These are type II or III (IED) dipolar cycloadditions in which the electron density flows from the dipolarophile towards the dipole. The activation energy is high due to a significant distortion of the dipole in the transition state. Through the insights obtained in the present work, we aim to boost the interest towards this useful chemical transformation and provide a solid theoretical foundation to develop new reactions based on the acyl-isocyanide ylide dipole.

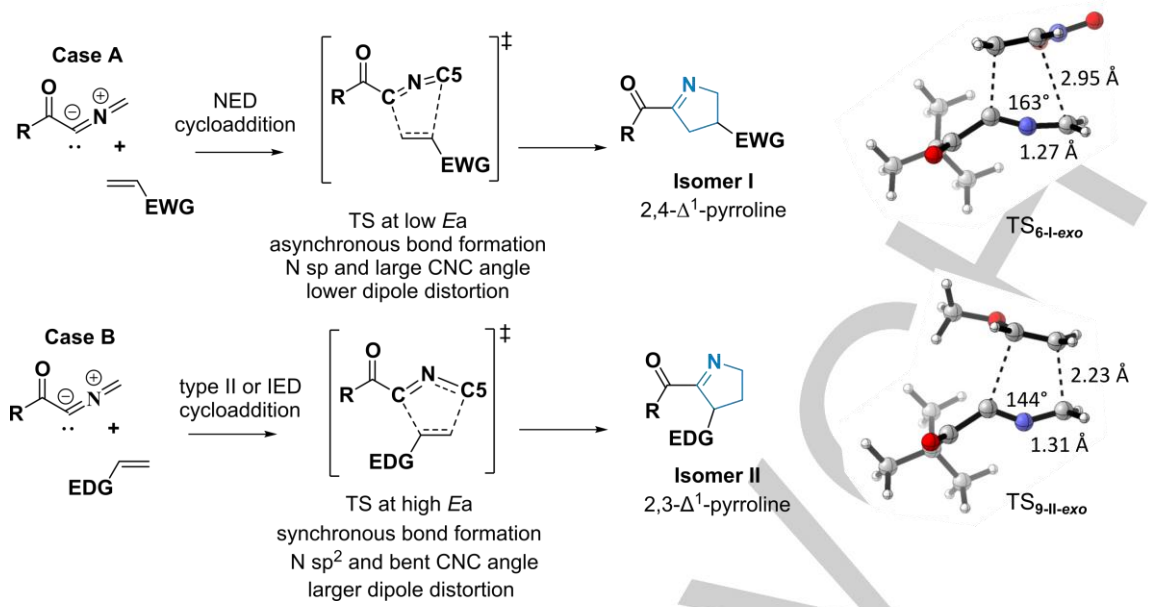

Figure 5. Two cases of 1,3-dipolar cycloadditions of acyl-isocyanide ylides to alkenes. The most favorable transition states for reactions **6** and **9** are depicted as examples. EDG: electron donating group, EGW: electron withdrawing group.

Acknowledgements

G.M.O.C. is grateful to VLIR-UOS for financial support of a Flemish-Cuba cooperation project (CU2018TEA458A101, recipient G.M.O.C., management, conceptualization and writing). J.E.A.R., D.H.C. and R.G.A. acknowledge the support of the International Fund and Project Management Office from the Ministry of Science, Technology and Environment, Republic of Cuba (project PN223LH010-02X, recipient J.E.A.R., experiments, data analysis and writing, and D.H.C. and R.G.A., revision of manuscript and technical support). R.V.L. acknowledges the use of Tier2 computational resources and services provided by the Shared ICT Services Centre funded by the Vrije Universiteit Brussel, the Flemish Supercomputer Center (VSC), and FWO. R.V.L. thanks FWO for the Ph.D. fellowships received (1185221N, recipient R.V.L., experiments, writing, data analysis and visualization). E.V.V.d.E. is thankful to "RUDN University Strategic Academic Leadership Program" for financial support. The publication has been prepared with the support of the «RUDN University Strategic Academic Leadership Program» (recipient EVdE, supervision and writing). F.D.P. wishes to acknowledge the Vrije Universiteit Brussel for the support through a Strategic Research Program (supervision and revision of manuscript).

Keywords: 1,3-dipolar cycloaddition • acyl isocyanide ylides • Activation Strain Model • regioselectivity • Density Functional Theory

[1] a) M. Breugst, H.-U. Reissig, *Angew. Chem. Int. Ed.* **2020**, *59*, 12293-12307. b) S. E. Beutick, P. Vermeeren, T. A. Hamlin, *Chem. Asian J.* **2022**, e202200553.

[2] V. V. Rostovtsev, L. G. Green, V. V. Fokin, K. B. Sharpless, *Angew. Chem. Int. Ed.* **2002**, *41*, 2596-2599.

[3] a) F. Himo, T. Lovell, R. Hilgraf, V. V. Rostovtsev, L. Noodleman, K. B. Sharpless, V. V. Fokin, *J. Am. Chem. Soc.* **2005**, *127*, 210-216. b) B. C. Boren, S. Narayan, L. K. Rasmussen, L. Zhang, H. Zhao, Z. Lin, G. Jia, V. V. Fokin, *J. Am. Chem. Soc.* **2008**, *130*, 8923-8930. c) N. K. Devaraj, M. G. Finn, *Chem. Rev.* **2021**, *121*, 6697-6698.

[4] P. Thirumurugan, D. Matosiuk, K. Jozwiak, *Chem. Rev.* **2013**, *113*, 4905-4979.

[5] a) L. Reguera, Y. Méndez, A. R. Humpierre, O. Valdés, D. G. Rivera, *Acc. Chem. Res.* **2018**, *51*, 1475-1486. b) A. Massarotti, F. Brunelli, S. Aprile, M. Giustiniano, G. C. Tron, *Chem. Rev.* **2021**, *121*, 10742-10788. c) M. Giustiniano, A. Basso, V. Mercalli, A. Massarotti, E. Novellino, G. C. Tron, J. Zhu, *Chem. Soc. Rev.* **2017**, *46*, 1295-1357. d) I. Ugi, B. Werner, A. Dömling, *Molecules* **2003**, *8*, 53-66.

[6] a) Y. Zhu, J.-Y. Liao, L. Qian, *Front. Chem.* **2021**, *9*, 670751. b) I. V. Efimov, L. N. Kulikova, D. I. Zhilyaev, L. G. Voskressensky, *Eur. J. Org. Chem. Chemistry* **2020**, *2020*, 7284-7303.

[7] W.-S. Tian, T. Livinghouse, *J. Chem. Soc. Chem. Commun.* **1989**, 819-821.

[8] P. de March, M. el Arrad, M. Figueredo, *J. Font. Tetrahedron* **1998**, *54*, 11613-11622.

[9] N. S. Medran, A. La-Venia, S. A. Testero, *RSC Adv.* **2019**, *9*, 6804-6844.

[10] a) W. C. Herndon, *Chem. Rev.* **1972**, *72*, 157-179. b) B. T. Worrell, J. A. Malik, V. V. Fokin, *Science* **2013**, *340*, 457-460.

[11] a) K. Fukui, T. Yonezawa, H. Shingu, *J. Chem. Phys.* **1952**, *20*, 722-725. b) K. Fukui, T. Yonezawa, C. Nagata, H. Shingu, *J. Chem. Phys.* **1954**, *22*, 1433-1442. c) H. G. O. Becker, *J. Prakt. Chem.* **1978**, *320*, 879-880.

[12] R. G. Parr, W. Yang, *J. Am. Chem. Soc.* **1984**, *106*, 4049-4050.

[13] F. M. Bickelhaupt, K. N. Houk, *Angew. Chem. Int. Ed.* **2017**, *56*, 10070-10086.

[14] a) F. M. Bickelhaupt, E. J. Baerends in *Reviews in Computational Chemistry* (Eds.: K.B. Lipkowitz, D. B. Boyd) Wiley, Hoboken, **2000**, 1-86. b) P. Vermeeren, S. C. C. van der Lubbe, C. Fonseca Guerra, F. M. Bickelhaupt, T. A. Hamlin, *Nat. Prot.* **2020**, *15*, 649-667.

[15] a) C. Morera-Boado, M. Martínez-González, R. A. Miranda-Quintana, M. Suárez, R. Martínez-Álvarez, N. Martín, J. M. G. de la Vega, *J. Phys. Chem. A* **2016**, *120*, 8830-8842. b) R. A. Miranda-Quintana, M. M. González, D. Hernández-Castillo, L. A. Montero-Cabrera, P. W. Ayers, C. Morell, *J. Mol. Model.* **2017**, *23*, 236. c) R. Jasiński, E. Dresler, *Organics* **2020**, *1*, 49-69. d) M. Martínez-González, D. Hernández-Castillo, L. A. Montero-Cabrera, R. A. Miranda-Quintana, *Int. J. Quant. Chem.* **2017**, *117*, e25444. e) A. Sengupta, B. Li, D. Svatunek, F. Liu, K. N. Houk, *Acc. Chem. Res.* **2022**, doi: 10.1021/acs.accounts.2c00343.

[16] a) D. Svatunek, T. Hansen, K. N. Houk, T. A. Hamlin, *J. Org. Chem.* **2021**, *86*, 4320-4325. b) L. R. Domingo, M. J. Aurell, P. Pérez, J. A. Sáez, *RSC Adv.* **2012**, *2*, 1334-1342. c) L. Li, P. Mayer, D. S. Stephenson, A. R. Ofial, R. J. Mayer, H. Mayr, *Angew. Chem. Int. Ed.* **2022**, *61*, e202117047.

[17] GaussView, Version 6.1, Roy Dennington, T. A. Keith, J. M. Millam, Semichem Inc., Shawnee Mission, KS, **2016**.

[18] a) Y. Zhao, D. G. Truhlar, *Theor. Chem. Acc.* **2008**, *120*, 215-241. b) R. Ditchfield, W. J. Hehre, J. A. Pople, *J. Chem. Phys.* **1971**, *54*, 724-728.

[19] Gaussian 16, Revision A.03, M. J. Frisch, G. W. Trucks, H. B. Schlegel, G. E. Scuseria, M. A. Robb, J. R. Cheeseman, G. Scalmani, V. Barone, G. A. Petersson, H. Nakatsuji, X. Li, M. Caricato, A. V. Marenich, J. Bloino, B. G. Janesko, R. Gomperts, B. Mennucci, H. P. Hratchian, J. V. Ortiz, A. F. Izmaylov, J. L. Sonnenberg, D. Williams-Young, F. Ding, F. Lipparini, F. Egidi, J. Goings, B. Peng, A. Petrone, T. Henderson, D. Ranasinghe, V. G. Zakrzewski, J. Gao, N. Rega, G. Zheng, W. Liang, M. Hada, M. Ehara, K. Toyota, R. Fukuda, J. Hasegawa, M. Ishida, T. Nakajima, Y. Honda, O. Kitao, H. Nakai, T. Vreven, K. Throssell, J. A. Montgomery Jr., J. E. Peralta, F. Ogliaro, M. J. Bearpark, J. J. Heyd, E. N. Brothers, K. N. Kudin, V. N. Staroverov, T. A. Keith, R. Kobayashi, J. Normand, K. Raghavachari, A. P. Rendell, J. C. Burant, S. S. Iyengar, J. Tomasi, M. Cossi, J. M. Millam, M. Klene, C. Adamo, R. Cammi, J. W. Ochterski, R. L. Martin, K. Morokuma, O. Farkas, J. B. Foresman, D. J. Fox, Gaussian, Inc., Wallingford CT, 2016.

[20] S. E. Wheeler, K. N. Houk, *J. Chem. Theor. Comput.* **2010**, *6*, 395-404.

[21] A. V. Marenich, C. J. Cramer, D. G. Truhlar, *J. Phys. Chem. B* **2009**, *113*, 6378-6396.

[22] Y. Lan, L. Zou, Y. Cao, K. N. Houk, *J. Phys. Chem. A* **2011**, *115*, 13906-13920.

[23] E. Van Lenthe, E. J. Baerends, *J. Comput. Chem.* **2003**, *24*, 1142-1156.

[24] G. te Velde, F. M. Bickelhaupt, E. J. Baerends, C. Fonseca Guerra, S. J. A. van Gisbergen, J. G. Snijders, T. Ziegler, *J. Comput. Chem.* **2001**, *22*, 931-967.

[25] X. Sun, T. M. Soini, J. Poater, T. A. Hamlin, F. M. Bickelhaupt, *J. Comput. Chem.* **2019**, *40*, 2227-2233.

[26] E. R. Johnson, S. Keinan, P. Mori-Sanchez, J. Contreras-Garcia, A. J. Cohen, W. Yang, *J. Am. Chem. Soc.* **2010**, *132*, 6498-6506.

[27] R. A. Boto, F. Peccati, R. Laplaza, C. Quan, A. Carbone, J.-P. Piquemal, Y. Maday, J. Contreras-García, *J. Chem. Theor. Comput.* **2020**, *16*, 4150-4158.

[28] a) W. Humphrey, A. Dalke, K. Schulten, *J. Mol. Graph. Model.* **1996**, *14*, 33-38. b) CYLview20; Legault, C.Y., Université de Sherbrooke, **2020** (http://www.cylview.org).

[29] J. R.-G. Pedregal, P. Gómez-Orellana, J.-D. Maréchal, *J. Chem. Inf. Model.* **2018**, *58*, 561-564.

[30] a) N. Chéron, L. El Kaïm, L. Grimaud, P. Fleurat-Lessard, *J. Phys. Chem. A* **2011**, *115*, 10106-10112. b) F. La Spisa, G. C. Tron, L. El Kaïm, *Synthesis* **2014**, *46*, 829-841.

[31] W.-S. Huang, Y.-X. Zhang, C.-Y. Yuan, *Synth. Commun.* **1996**, *26*, 1149-1154.

[32] R. Sustmann, *Pure Appl. Chem.* **1974**, *40*, 569-593.

[33] B.-Y. Li, L. Voets, R. Van Lommel, F. Hoppenbrouwers, M. Alonso, S. H. L. Verhelst, W. M. De Borggraeve, J. Demaerel, *Chem. Sci.* **2022**, *13*, 2270-2279.

[34] For the values of the Hammet parameters σ_p used in this work see: C. Hansch, A. Leo, R. W. Taft, *Chem. Rev.* **1991**, *91*, 165-195.

[35] a) L. P. Hammett, *Chem. Rev.* **1935**, *17*, 125–136; b) L. P. Hammett, *J. Am. Chem. Soc.* **1937**, *59*, 96–103, c) O. Exner, J. Lakomý, *Collect. Czech. Chem. Commun.* **1970**, 35, 1371-1386, d) A. Hamid, R. K. Roy, *J. Phys. Chem. A* **2020**, *124*, 5775–5783; e) L. Wu, S.-Y. Tang, S. Zho, ACS Omega **2021**, *6*, 34904−34911.

10.1002/ejoc.202201028

WILEY-VCH

RESEARCH ARTICLE

Entry for the Table of Contents

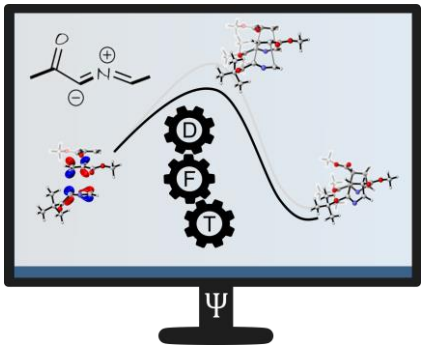

A toolbox of quantum chemical-based methods is used to elucidate the reactivity of acyl-isocyanide ylides in 1,3-dipolar cycloadditions. The theoretical analysis reveals two general modes of action depending on the electronic properties of the dipolarophile.

Institute and/or researcher Twitter usernames: @javialra97, @VanLommelRuben, @ALGC_VUB, @MolDesignS, @OjedaCarralero, @DavidHdez92.